



ORIGINAL ARTICLE

Contribution to the hydrogeology of the Lower Cretaceous aquifer in east Central Sinai, Egypt

Saad Y. Ghoubachi *

Desert Research Center, Egypt

Al-Quwaiyih Community College, Shaqra University, Saudi Arabia

Received 20 April 2010; accepted 24 May 2010

Available online 27 May 2010

KEYWORDS

Hydrogeology;
Lower Cretaceous aquifer;
Groundwater;
East Central Sinai;
Egypt

Abstract The Lower Cretaceous aquifer (Malha sandstone aquifer) represents the main aquifer in east Central Sinai. The hydrogeological evaluation of the aquifer is based on the data of 14 selected deep wells. The objective of this paper aims to elucidate the hydrogeological characteristics of the Lower Cretaceous aquifer. The groundwater of Lower Cretaceous aquifer exists under confined conditions. The top surface of the Lower Cretaceous dips steeply towards the southwest direction. The average sand percent of the penetrated aquifer attains 54%. The groundwater flow direction of Lower Cretaceous aquifer is concentric to the center of study area related to the influence of the graben block. The general hydraulic gradient reaches 0.0011 in southwestern portion, while it reaches 0.0028 in central portion of study area. The average effective porosity and transmissivity and hydraulic conductivity of the Lower Cretaceous aquifer are 17.3%, 416 m²/day and 1.4 m/day, respectively. They increase towards the northeast direction with increasing of the sand percentage.

Durov diagram plot revealed that the groundwater has been a final stage evolution represented by a NaCl water type. The groundwater salinity increases towards the central portion of study area coinciding with groundwater flow. The groundwater salinity of the Lower Cretaceous aquifer is brackish water and varies from 2510 to 5256 ppm. It is unsuitable for drinking and domestic purposes.

© 2010 King Saud University. Production and hosting by Elsevier B.V. All rights reserved.

* Address: Al-Quwaiyih Community College, Shaqra University, Saudi Arabia. Tel.: +966 504364882.

E-mail address: saadyounes@marktoob.com.



1. Introduction

The Lower Cretaceous aquifer in Central Sinai represents the main aquifer. During the last few decades groundwater exploitation in the Sinai Peninsula has increased dramatically, mainly due to an increase in irrigated agriculture, tourism and industry. To meet the needs of drinking water for future generations, sustainable watershed management is essential for drinking water supply especially in semiarid areas, and requires a more detailed knowledge about the hydrogeology of the Lower Cretaceous aquifer. The Lower Cretaceous aquifer in the study area is considered to be the most important

groundwater reservoir in this area providing large amounts of water for the development of this promising area. This paper describes the hydrogeology of Lower Cretaceous aquifer in east Central Sinai.

The study area lies in the east Central Sinai and extended to the eastern Egyptian border (Fig. 1). It is located between longitudes 34°00'E and 34°30'E and latitudes 30°15'N and 30°45'N.

This area lies in an arid transitional climatic zone between the influence of the Sahara and the Mediterranean systems of North Africa. The rainfall attains a relatively low precipitation

ranges between 14 and 26 mm/year, however, the pluvial paleo-climate has its effect on the hydrologic regime of the area. The average temperature ranges between 8 and 15 °C in winter and between 21 and 27 °C in summer. The natural evaporation ranges between 6.5 and 15 mm/day in winter and summer, respectively (WRRI, 1995).

The present work aims to elucidate the hydrogeological characteristics of the Lower Cretaceous aquifer. This depends on the new hydrogeological and hydrologic data for 14-deep drilled wells as well as hydrochemical analyses of representative groundwater samples.

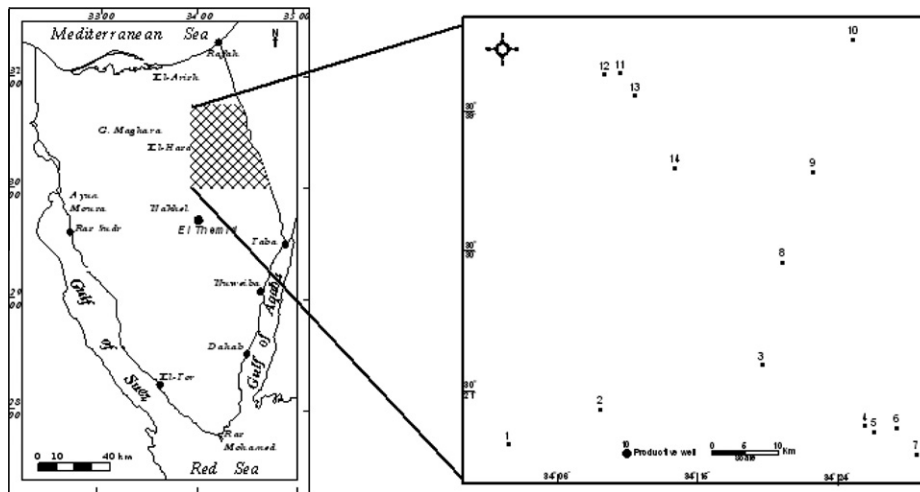


Figure 1 Location and well location map of study area.

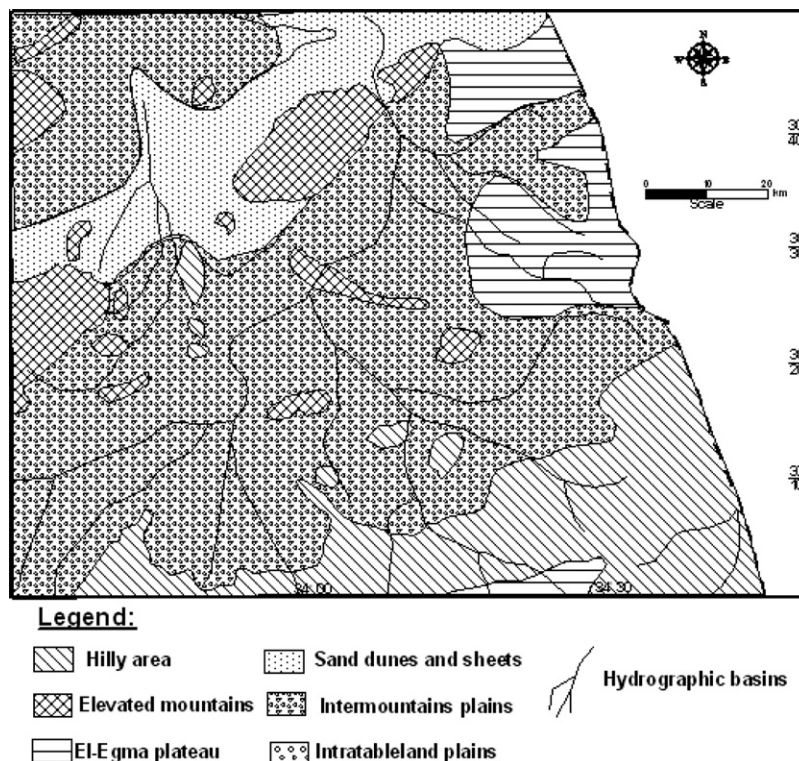


Figure 2 The main geomorphological units of study area (after Hassanin, 1997).

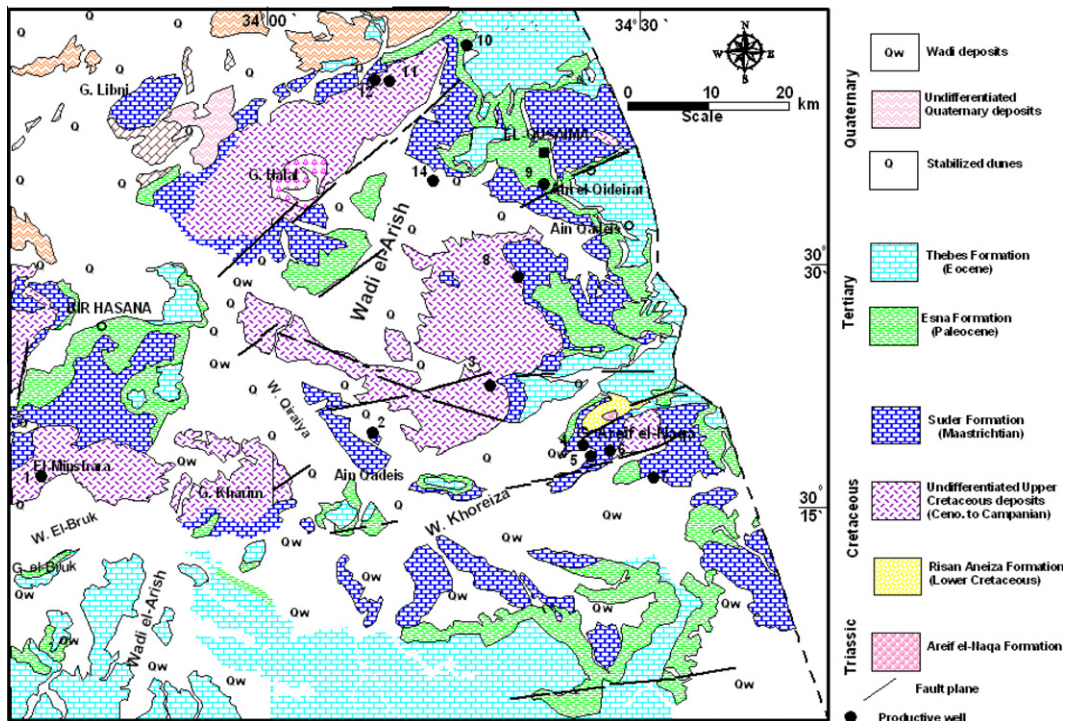


Figure 3 Geological map of the study area (modified after CONOCO, 1987).

Era	Age	Formation	Thick (m)	Lithology	Lithological description	
Cenozoic	Quaternary		variable		Wadi deposits, sand, silt and carbonate	
	Eocene	Middle	Samalut	60		Shallow marine limestone with Nummulite + Glauconite
		Lower	Egma	200		Moderately bedded marine chalky limestone with chert bands
	Paleocene	Esna	40			Greenish grey marine shale
Mesozoic	Cretaceous	Upper	Sudr	100		Marine chalk with thin shale intercalations
			Matallah	140		Marine sandstone, marl and shale
			Wata	100		Fossiliferous limestone with marl intercalations
			Halal	100		Limestone
	Lower	Malha	340			White sandstone locally conglomerate
		Jurassic	Raqabah	40		White sandstone locally conglomerate
		Triassic	Oisaib	40		Interbedded friable sandstone with mudstone

Figure 4 Stratigraphic succession in study area (modified after WRRI, 1995).

1.1. Geomorphological setting

Several geomorphological studies have been made for individual parts of the investigated area. The most important studies

were made by Shata (1960), Said (1962), Hammad (1980), and Hassanin (1997). The surface of study is geomorphologically subdivided into distinct geomorphic units according to Hassanin (1997) as shown in Fig. 2.

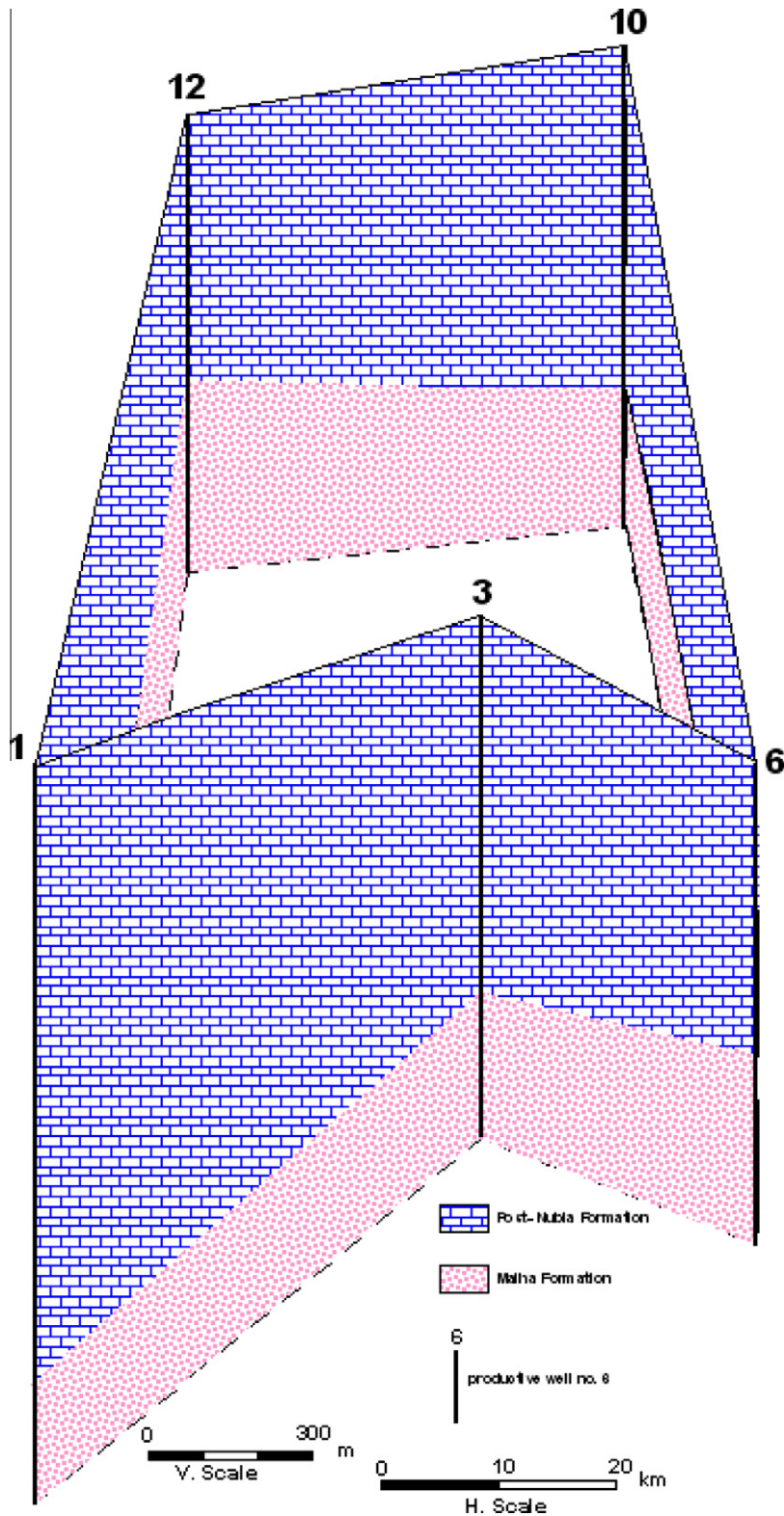


Figure 5 Panel diagram showing subsurface in east Central Sinai.

1.1.1. The watershed areas (highlands)

These units receive the rainwater and classified into the Egma plateau, hilly area and elevated mountain. El-Egma plateau represents the principal watershed area in the study area. This

plateau is mainly composed of Lower Eocene chalky limestone with chart bands. Its surface is dissected by many consequent drainage lines that form the intake portion of Wadi El-Arish.

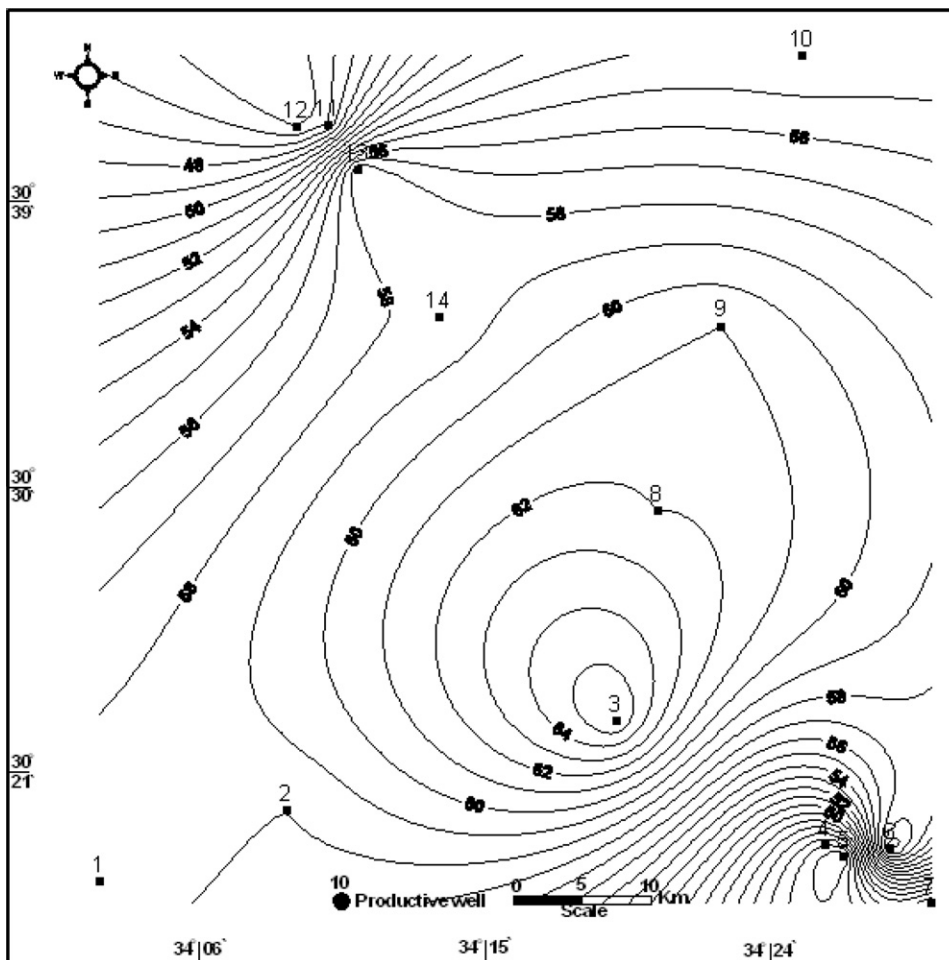


Figure 6 Sand percent contour map of the Lower Cretaceous.

Table 1 Hydrogeological data of some wells tapping Lower Cretaceous aquifer.

Well No.	Well name	Total depth (m)	Water level (masl)	Screen interval (m)		Thickness (m)	Sand (%)	Top surface Lower Cretaceous aquifer (masl)	Salinity (ppm)
				From	To				
1	Khream	1375	174	1130	1375	245	59	-875	5283
2	El-Batohy	1032	165	820	1032	212	58	-503	2794
3	El-Biraq	973		700	970	270	66	-265	3828
4	Arif El-Naqa1	877		550	877	327	44	-15	2809
5	Arif El-Naqa2	870		550	870	320	42	-25	
6	Khareza	902	155	650	902	252	60	-101	
7	Arif El-Naqa19a	900	154	600	900	300	45	-101	
8	Grur	860	150	660	860	200	62	-190	3653
9	Gaifi	842	140	690	830	140	60	-150	5285
10	Sabha	900	151	700	900	200	54	-192	2510
11	Halal 1	850	163	550	850	300	46	-187	
12	Halal 2	850		550	850	300	45	-150	2880
13	Monbath	1004		750	1004	254	59	-464	
14	Hodaybia	850	115	620	850	222	58	-210	4697

Hilly areas constitute very prominent land features represented by the folded blocks. These folded blocks are formed of elevated and isolated mountains arranged in several rows running in northeast southwest direction (Syrian Arc trend). Numerous wadis that are mostly developed along the fault lines excavate these mountains. Some of these wades have fair groundwater supplies and favorable soil potentialities.

An elevated mountain reveals wide variations in its size and composition depending upon the local structural setting and the weathering processes. The core of the elevated mountain exposes of Triassic formation (Gebel Arif El-Naqa) and Lower Cretaceous sandstone (Gebel El-Halal).

1.1.2. The water collectors areas

The water collectors are represented by the lowland areas (hydrographic system, intermountains plains and sand dunes and sheets). These lowland areas store and collect the surface water and recharge the groundwater.

2. Geological setting

The main surface geology is described in the geological map of Sinai at a scale 1:500,000, performed by (CONOCO, 1987) and is shown in Fig. 3. The study area is mostly covered by Quaternary deposits composed of alluvium and sand dunes deposits.

The Lower Eocene Thebes Formation extensively covers El-Egma plateau, which is locally called Egma limestone. Paleocene deposits including Esna Shale Formation, which is composed of marly shale. The Upper Cretaceous is represented by Sudr Formation, which is composed of chalk of Maastrichtian age, Duwai Formation composed of alternated carbonate and clastic of Campanian age, Matullah Formation, which is composed of limestone of Conician–Santonian age, and Wata Formation, composed of dolomitic limestone of Conician–Turonian deposits. Halal Formation that belongs to Cenomanian age is composed of limestone (Fig. 4). Its stratigraphy and structures are strongly interrelated and have a great impact on the groundwater quality and potential.

The geology of Central Sinai is delineated by different authors among them are: Shata (1956), Said (1962, 1990), El-Shazly et al. (1974), El-Ghazawi (1989), Hassanin (1997) and Ali (2006).

Lower Cretaceous is represented by Malha Formation, which is composed sandstone and clay succession that were formerly lumped under the Nubia sandstone. In other word, the sandstone succession of Lower Cretaceous Formation in the south gradually changes in facies into shaly and calcareous sequence in north which is locally called as Risan Aneiza Formation (Said, 1971). The Triassic sediments outcrop only in the core of Gebel Arief El-Naqa. Areif El-Naqa For-

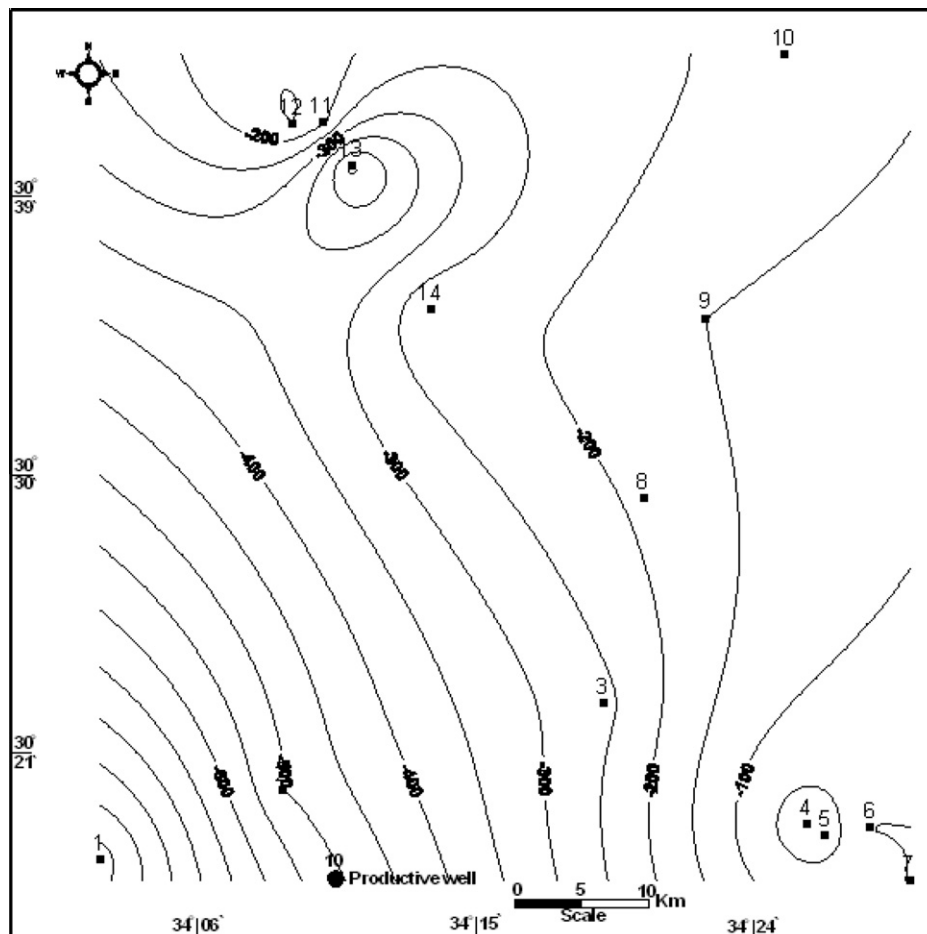


Figure 7 Top surface map of Lower Cretaceous aquifer related to Sea Level.

mation is composed of sandstone with interbeds of variegated shale.

The structural pattern of east Central Sinai shows that folding is much more pronounced than faulting. The area of study

displays the strongly folded province (Shata, 1956). This structure plays a great role to the influence on the hydrogeologic setting. This is reflected on the groundwater occurrence, replenishment, movement and potentialities. This belt is char-

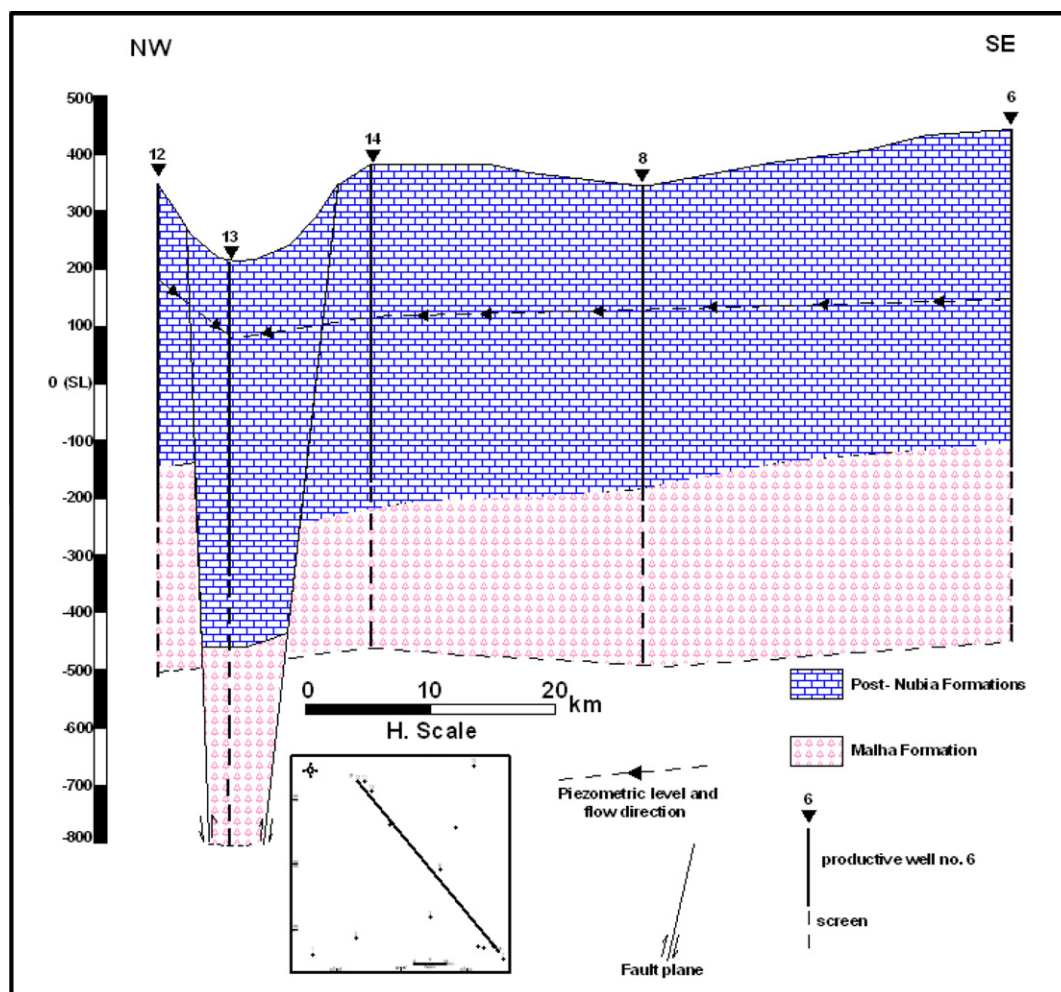


Figure 8 Hydrogeological cross-section in study area.

Table 2 Hydrologic parameters of some wells in study area.

Well No.	Drawdown (m)	Transmissivity (m^2/day)	Hydraulic conductivity (m/day)	Effective porosity (%)	Productivity (m^3/h)
1	47.57	110	0.94	15.5	39
2	4.12		1.2	16.5	50
3			1.3	17	
4	3.87	414	1.5	17.5	75
5			1.3	17	
6			1.5	17.5	
7		399	1.64	18	20
8	1.23	575	1.64	18	39
9	1.5	493	2.05	19	45
10	8.5	488	1.5	17.5	44
11			1.3	17	
12	13.12		1.53	17.7	50
13			1.3	17	
14	2.47		1.3	17	51

acterized by extensive anticline mountain arranged in parallel lines oriented in ENE–WSW direction separated by vast synclinal flat plains (Hassanin, 1997). Faulting is common and has a pronounced influence on the local topographic and groundwater flow.

A panel diagram (Fig. 5) is constructed for the subsurface of Lower Cretaceous Formation (Nubia Formation) and post-Nubia Formations in the study area. This diagram shows that the thickness of post-Nubia Formations increases towards the southwest direction, while the thickness of Lower Cretaceous Formation decreases in the same direction.

3. Hydrogeological setting

Lower Cretaceous aquifer in the study area is represented by Malha sandstone aquifer. It is considered as the main aquifer in the investigated area. Accordingly, the evaluation of this aquifer in the study area is very important for the development of this area.

Lower Cretaceous aquifer is directly rested on the Jurassic sandstone aquifer (Ali, 2006). The Jurassic aquifer is characterized by high groundwater salinity. The concerned aquifer is mainly composed of vari-colored, medium to coarse-grained sandstone with dark, sticky claystone interbeds. It was deposited under continental fluvial environment.

The penetrated thickness of the investigated aquifer ranges from 140 m (well no. 9) to 327 m (well no. 4). The sand percentage of the penetrated thickness of this aquifer varies from 42% (well no. 5) to 66% (well no. 3) and its average reaches 54%. Generally, this sand percentage of this aquifer increases towards the east direction (Fig. 6). The total depth of the drilled wells ranges from 842 m in well no. 9 to 1375 m in well no. 1 (Table 1). The top surface of Lower Cretaceous aquifer is recorded at depths ranging between -875 m under sea level at well no. 1 and -15 m at well no. 4 (Table 1). The top surface of the Lower Cretaceous dips steeply towards the southwest direction (Fig. 7).

The groundwater of Lower Cretaceous aquifer exists under confined conditions. This aquifer is hydraulically connected with both the underlying Jurassic sandstone aquifer and overlying post-Nubia. This is attributed to the faulting, where the present aquifer comes in contact with each other as a result of faulting displacement (Fig. 8). The productivity of the wells tapping Lower Cretaceous sandstone aquifer varies from $20 \text{ m}^3/\text{h}$ (well no. 7) to $75 \text{ m}^3/\text{h}$ (well no. 4). The drawdown of the concerned aquifer ranges from 1.23 m (well no. 8) to 47.57 m (well no. 1) as shown in Table 2. The higher drawdown is attributed to the aquifer in this well has low effective porosity. On the other hand, the lower drawdown in well no. 8 is related

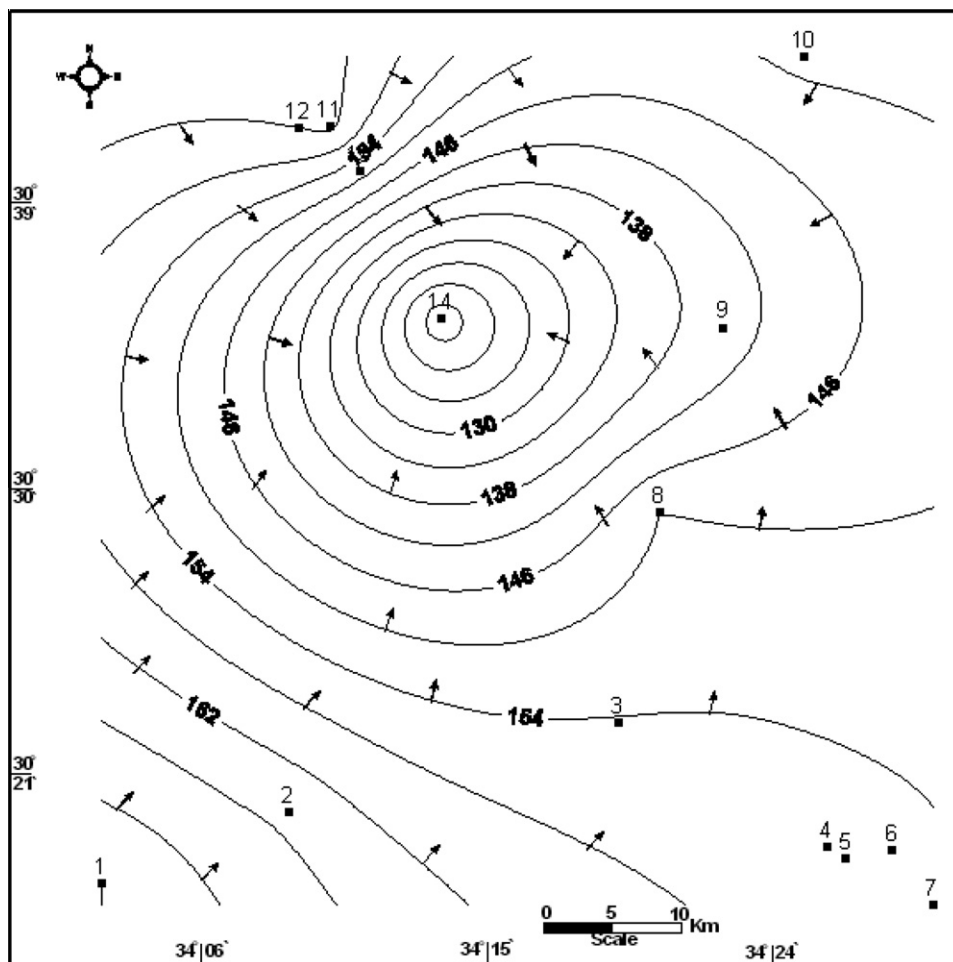


Figure 9 Piezometric level map of the Lower Cretaceous aquifer.

to the aquifer in this well has high sand percentage and effective porosity.

3.1. Groundwater flow

The Lower Cretaceous sandstone aquifer is detected in all the drilled wells in the study area and represents the main exploitable aquifer. The piezometric surface of the present aquifer ranges between 174 m (asl) in well no. 1 at southwestern portion of the study area and 115 in well no. 14 at central portion of the investigated area. The piezometric contour map reveals that the groundwater flow directions are concentric to the center of the study area (Fig. 9). This is attributed to the influence of the graben block (Fig. 8). The general hydraulic gradient reaches 0.0011 in southwestern portion, while it reaches 0.0028 in central portion of the study area. The steep hydraulic gradient of Lower Cretaceous sandstone aquifer in the central area than other areas is attributed to the influence of graben block.

3.2. Hydrologic properties

The hydrologic properties of the Lower Cretaceous aquifer in east Central Sinai area are determined based on laboratory techniques. They comprise the following (Table 2):

3.2.1. Effective porosity (Φ_{eff})

The effective porosity of the investigated aquifer is determined from the geophysical well logging data applying Archie equation (1942). The effective porosity is obtained by the following equation:

$$\Phi_{eff} = (5400Rt * Rw)^{1/2} \quad (\text{in sodium chloride water type})$$

where Φ_{eff} is the effective porosity in percent, Rt is the true resistivity in Ω m and Rw is the formation of water resistivity in Ω m.

The true resistivity (Rt) is determined by correction of the long resistivity $\log(R_{64''})$ or (R_{LLD}) and short normal resistivity $\log(R_{16''})$ or (R_{LLS}). The true resistivity (Rt) is obtained by the following equation: $Rt = 1.7R_{LLD} - 0.7R_{LLS}$ (if $R_{LLD} > R_{LLS}$). The effective porosity of the investigated aquifer varies from 15.5% (well no. 1) to 19% (well no. 9) as shown in Table 2, with an average effective porosity reaches 17.3%. The effective porosity of the studied aquifer increases towards the northeast direction with increasing of the sand percentage as shown in Fig. 10.

3.2.2. Transmissivity

The transmissivity of the concerned aquifer is estimated by the analyses of the obtained data of the pumping test (WRI, 2001). The original raw data of pumping test which are ob-

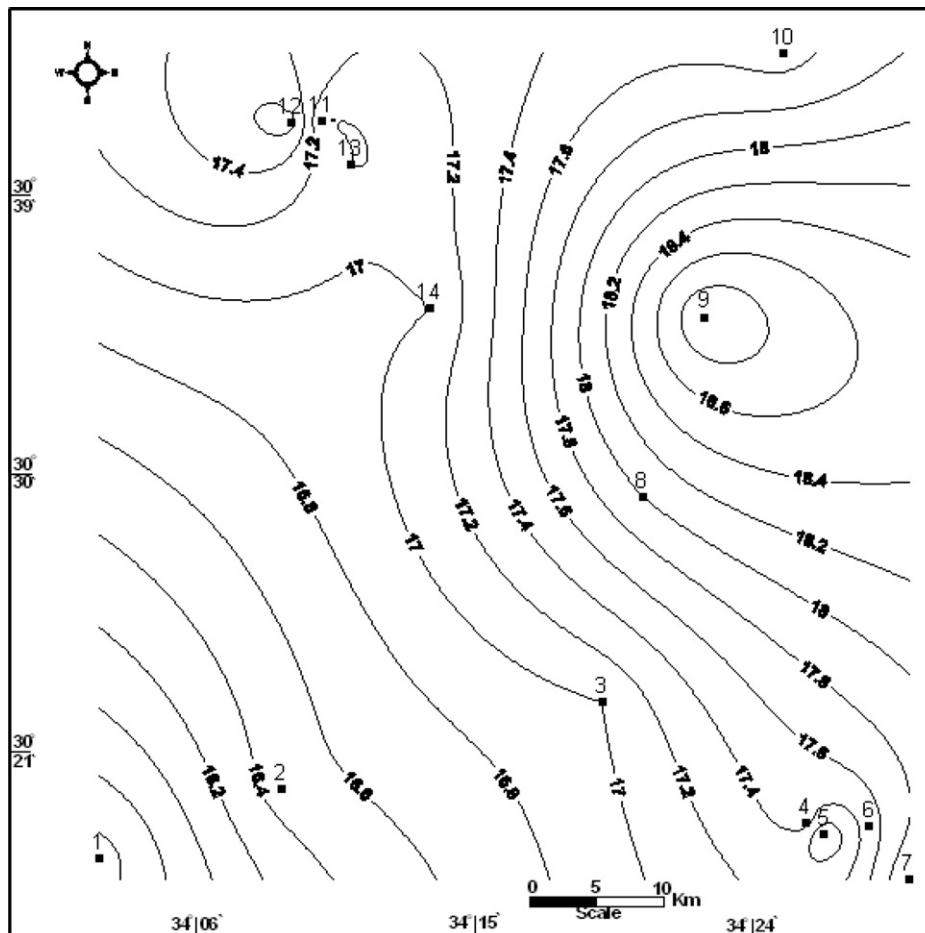


Figure 10 Porosity contour map of the Lower Cretaceous aquifer.

tained through the present work are analyzed by using Cooper and Jacob method (1946) and GWW computer program. Transmissivity of the investigated aquifer is calculated for five wells distributed in the study area (Table 2). The analysis of constant discharge test was executed using Cooper and Jacob method. This method was presented by Cooper and Jacob (1946) and discussed by Kruseman and de Ridder (1990). The assumptions of this method are satisfied by the present hydrogeological conditions in the studied area.

The calculated transmissivity of the concerned aquifer ranges between about 110 m²/day (well no. 1) and 575 m²/day (well no. 8) as shown in Table 2 with averages of about 416 m²/day. The low transmissivity of well no. 10 is attributed to this well have low sand percent. On the other hand, the high transmissivity of well no. 8 is due to this well has high saturated thickness and sand percent. Distribution transmissivity map is compiled for the Lower Cretaceous sandstone aquifer (Fig. 11). It reveals that the transmissivity of the concerned aquifer increases towards the northeast direction with increasing of sand percent and effective porosity.

3.2.3. Hydraulic conductivity

The hydraulic conductivity (K) of the aquifer is determined by the substitution of effective porosity in Marotz equation

(1968). The effective porosity is calculated by using Arachi equation. The hydraulic conductivity is obtained by the following equation:

$$\Phi_{\text{eff}} = 0.462 + 0.045 \ln K$$

where Φ_{eff} is the effective porosity in decimal and K is the hydraulic conductivity in cm/s.

The hydraulic conductivity of the investigated aquifer ranges from 0.94 m/day in well no. 1 (southwestern portion) to 2.05 m/day in well no. 9 (northeastern portion) and its average attains 1.4 m/day. It increases due northeast (Fig. 12) with increasing of effective porosity and sand percentage.

4. Hydrochemical characteristics

The hydrochemical characteristics of Lower Cretaceous aquifer depend on the analyses of nine groundwater samples (Table 3). Those will be described herein through the following.

4.1. The groundwater salinity

The groundwater salinity of the studied aquifer reveals a great variation reflecting the effect of the facies changes, the structural effect and the hydrochemical processes. It varies from

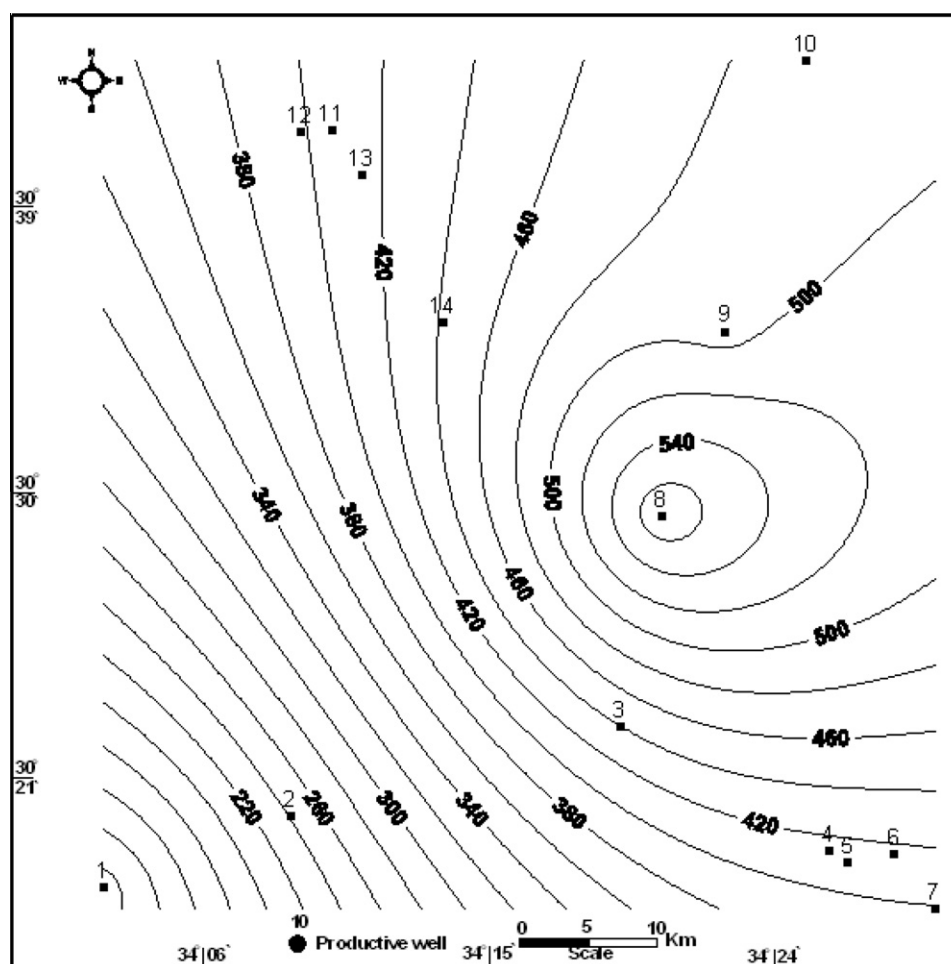


Figure 11 Transmissivity distribution map of Lower Cretaceous aquifer.

Table 3 Chemical analyses of the studied groundwater samples.

Well No.	EC ($\mu\text{mhos/cm}$)	TDS (ppm)	Units	Cations				Total (epm)	Anions			Total (epm)
				Ca ²⁺	Mg ²⁺	Na ⁺	K ⁺		HCO ₃ ⁻	SO ₄ ²⁻	Cl ⁻	
1	8800	4364	ppm	660	109.4	1021	38	87.3	152	1000	2379	90.4
			epm	32.93	9	44.4	0.97		2.49	20.82	67.09	
			epm %	37.72	10.31	50.86	1.11		2.76	23.03	74.21	
2	4650	2694	ppm	204	196.95	460	60	47.91	426	500	1060	47.19
			epm	10.18	16.2	20	1.54		6.89	10.41	29.89	
			epm %	21.25	33.81	41.74	3.2		14.6	22.06	63.34	
3	6200	3778	ppm	420	328	400	56	66.75	248	1000	1450	65.77
			epm	20.96	26.97	17.39	1.43		4.06	20.82	40.89	
			epm %	31.4	40.4	26.05	2.15		6.18	31.65	62.17	
4	4550	2809	ppm	201	70.1	675	23	47.73	302.6	739	950	47.14
			epm	10.03	5.77	29.35	0.59		4.96	15.39	26.79	
			epm %	21.93	12.61	64.18	1.29		10.52	32.64	56.84	
5	5656	3242	ppm	272	106	760	20	55.84	398.9	380	1505	56.89
			epm	13.57	8.72	33.04	0.51		6.54	7.91	42.44	
			epm %	24.3	15.62	59.17	0.91		11.49	13.9	74.61	
8	6200	3634	ppm	320	225	640	20	62.81	220	1000	1318.76	61.62
			epm	15.97	18.5	27.83	0.51		3.61	20.82	37.19	
			epm %	25.42	29.46	44.31	0.81		5.86	33.79	60.35	
9	9100	5256	ppm	380	364.8	996	20	92.77	172	1050	2360.46	91.24
			epm	18.96	30	43.3	0.51		2.82	21.86	66.56	
			epm %	20.44	32.34	46.67	0.55		3.09	23.96	72.95	
10	4250	2510	ppm	224	87.58	560	40	43.75	228	525	960	41.74
			epm	11.18	7.2	24.35	1.02		3.74	10.93	27.07	
			epm %	25.55	16.46	55.66	2.33		8.95	26.19	64.86	
12	4850	2880	ppm	78	76.4	878	40	49.37	332	435	1207.4	48.55
			epm	3.89	6.28	38.18	1.02		5.44	9.06	34.05	
			epm %	7.88	12.73	77.32	2.07		11.20	18.66	70.14	

2510 ppm (well no. 10) to 5256 ppm (well no. 9), where it is brackish water. The low groundwater salinity is related to this well which is located in the upthrown side of the fault (Fig. 8), where the faults are generally accompanied by the presence of best groundwater especially on their upthrown sides (Youssef and El-Saady, 1964). The high salinity of well no. 9 is essentially attributed to this well which is located in graben block, where the groundwater moves due graben and increases salinity with flow direction. The constructed groundwater salinity for this aquifer reveals an increase of groundwater salinity due central of the study area with groundwater flow direction (Fig. 13).

4.2. Ion dominance

The ion concentrations, the sodium and chloride dominate the other ions in the majority of the groundwater samples. The sequence of ion dominance of both cations and anions in the water follows the order $\text{Na}^+ > \text{Mg}^{2+} (\text{Ca}^{2+}) > \text{Ca}^{2+} (\text{Mg}^{2+})$ and $\text{Cl}^- > \text{SO}_4^{2-} > \text{HCO}_3^-$. So, the chemical water type is sodium chloride. The magnesium and calcium exceed the sodium ions only in well no. 3 with the abundance of the chloride among the anions. Consequently, the water chemical type in this case becomes magnesium chloride in well no.

4.3. The hypothetical salt

The hypothetical salt assemblages: the dissolved salts in the groundwater of the studied aquifer are grouped into two assemblages of hypothetical salts combinations as the following (Table 4):

Group I: NaCl, MgCl₂, CaCl₂, CaSO₄ and Ca(HCO₃)₂. This assemblage has been encountered in the majority of the wells.

Group II: NaCl, MgCl₂, MgSO₄, CaSO₄ and Ca(HCO₃)₂. Such salts are only found in wells nos. 1 and 4.

It is noticed that the above two groups comprise MgCl₂ and CaCl₂ salts of marine origin. This is attributed to the present aquifer which is hydraulically connected with post-Nubia limestone aquifers rich in marine salts.

4.4. Hydrochemical facies

Durov's diagram (Durov, 1948) gives more information on the hydrochemical facies and the evolution of groundwater quality. It helps in identifying hydrochemical facies or water types and can indicate mixing of different water types, ion-exchange and reverse ion-exchange processes. The expanded Durov's

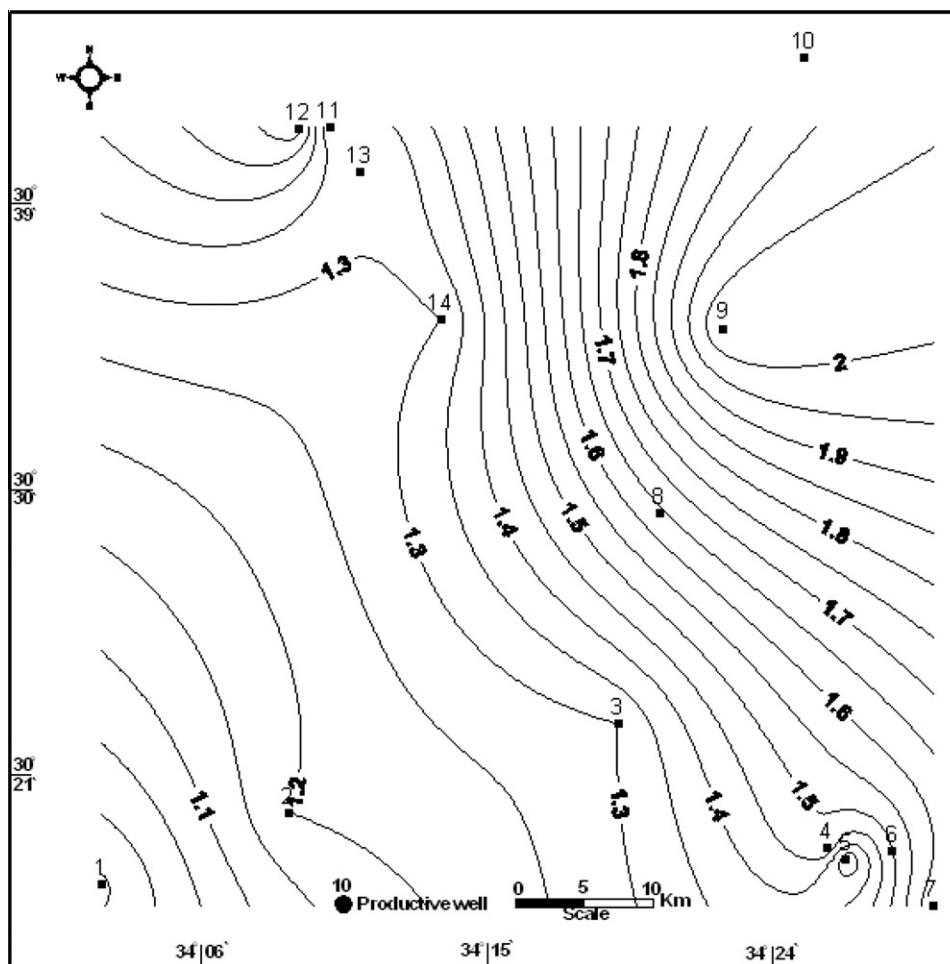


Figure 12 Hydraulic conductivity map of Lower Cretaceous aquifer.

diagram (Fig. 14) was used to help in classifying groundwater types and identifying hydrochemical facies in the study area.

The groundwater types of the Lower Cretaceous aquifer were formed to belong to two hydrochemical facies, according to their order of importance; the types were 8 and 9. Type 8 is chloride anion, and has no dominant cation (wells 2, 3, 8 and 9). The last type 9 is chloride and sodium ions as dominant (wells 1, 4, 10 and 12) indicating the end point water.

4.5. Groundwater quality

Different chemical quality standards have been established for evaluating the water suitability for drinking, domestic, livestock and irrigation uses (Table 5). In the present study the groundwater suitability for different uses is based on the concentration of its major ion constituents.

4.5.1. Groundwater quality for drinking and domestic uses

The evaluation of groundwater quality for drinking and domestic uses is attempted depending on some international standards, suggested by the World Health Organization (WHO, 1993). The groundwater samples have total dissolved solids (TDS) that exceed the safe limits for drinking

use. So, the groundwater in the area is not suitable for drinking.

4.5.2. Groundwater quality for livestock and poultry uses

The evaluation of the groundwater for livestock and poultry uses is based on the National Academy of Science (1972) limitations. According to the classification of National Academy of Science (1972), the groundwater in the study area can be classified into two main categories: (a) very satisfactory (TDS 1000–3000 mg/l) for the groundwater in the wells nos. 2, 4, 10 and 12. (b) Satisfactory water for livestock and poor for poultry (TDS 3000–5000 mg/l) in wells nos. 3, 5 and 8. On the other hand, the groundwater in wells nos. 1 and 9 can be used with reasonable safety for livestock and not acceptable for poultry.

4.5.3. Groundwater quality for irrigation purposes

Several chemical constituents affect water suitability for irrigation from which the total concentration of the soluble salts and the relative proportion of sodium to calcium and magnesium. Moreover suitability of water for irrigation is depended on the effect of some mineral constituents in the water on both the soil and the plant.

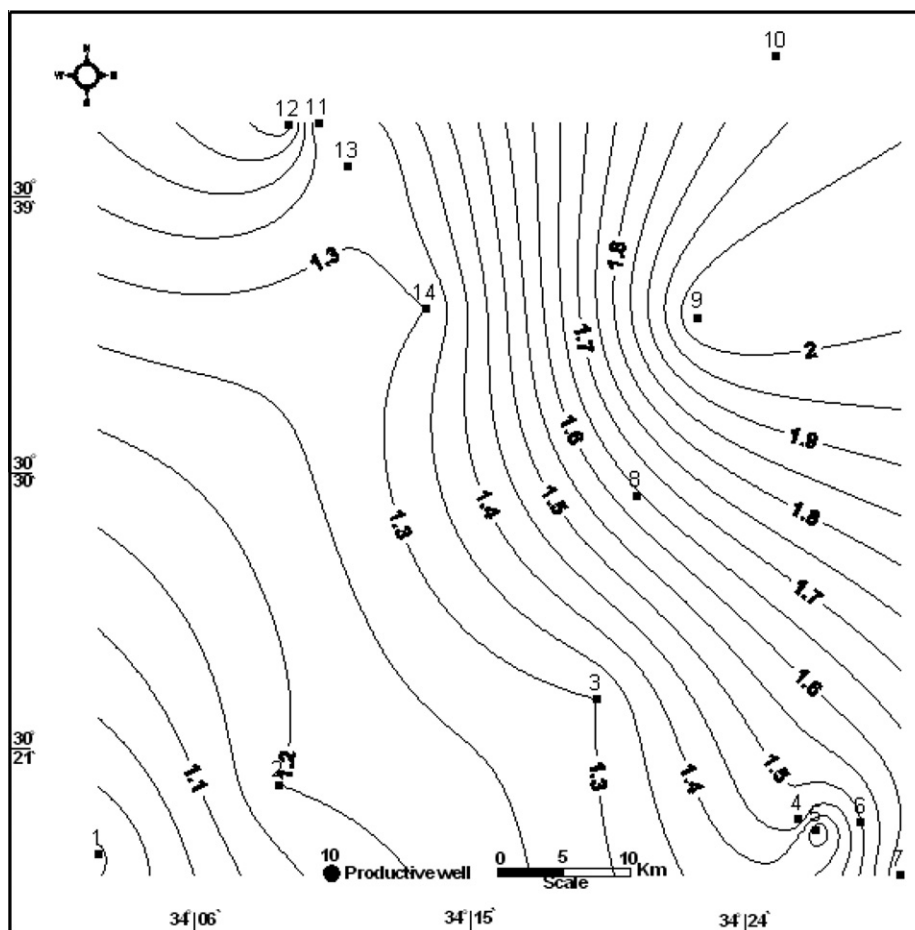


Figure 13 Distribution map of groundwater salinity of Lower Cretaceous aquifer.

Table 4 Hydrochemical characteristics of the groundwater samples.

Well No.	Hydrochemical coefficients hypothetical salts							
	NaCl	MgCl ₂	ClCl ₂	MgSO ₄	CaSO ₄	Ca(HCO ₃) ₂	Mg(HCO ₃) ₂	Na ₂ SO ₄
1	51.97	10.31	11.93	–	23.03	2.76	–	–
2	44.94	18.4	–	3.66	–	21.25	11.75	–
3	28.2	33.97	–	6.43	25.22	6.18	–	–
4	56.84	–	–	12.61	11.4	10.52	–	8.63
5	60.08	14.53	–	1.09	12.81	11.49	–	–
8	45.12	15.23	–	14.23	19.56	5.86	–	–
9	47.22	25.73	–	6.61	17.35	3.09	–	–
10	57.99	6.87	–	9.59	16.6	8.95	–	–
12	70.14	–	–	9.41	–	7.88	3.32	9.25

The groundwater quality in the area is evaluated also taken both the TDS and SAR values in consideration based of the irrigation water which based in turn on EC or TDS and SAR. The analyzed samples were plotted on US Salinity Laboratory Staff Method (1954) as shown in Fig. 15. The groundwater in the study area can be classified into three categories: (a) water of very high salinity and medium sodium (C4S2); this class includes groundwater sample no. 2, which presents an appreciable sodium hazard in the fine-textured soils especially

under low-leaching conditions. This water category is satisfactory for salt tolerant crops and soils of good permeability with special leaching. (b) Water of very high salinity and high sodium (C4S3); this class includes groundwater samples nos. 4 and 10. These groundwater samples are unsuitable for irrigation in most soils and require special soil management, good drainage, high leaching and organic matter additions. (c) Water of very high salinity and very high sodium (C4S4); this class includes groundwater sample no. 12. It is unsuitable for

Table 5 Groundwater quality of Lower Cretaceous aquifer.

Well No.	EC (mmhos/cm)	TDS (ppm)	SAR (epm)	Na (%)	Evaluation for		
					Drinking	Livestock and poultry	Irrigation by US salinity
1	8800	5284	9.9	52	Unsuitable	Excellent	C3S1
2	4650	2644	5.9	45	Unsuitable		C2S1
3	6200	3778	3.8	28	Unsuitable		C2S1
4	4550	2809	10.6	63	Unsuitable		C3S1
5	5656	3242	10	60	Unsuitable		C2S1
8	6200	3654	6.8	45	Unsuitable		C3S1
9	9100	5285	8.8	47	Unsuitable		C3S1
10	4250	2510	8.4	58	Unsuitable		C2S1
12	4850	2880	17.4	79	Unsuitable		C3S1

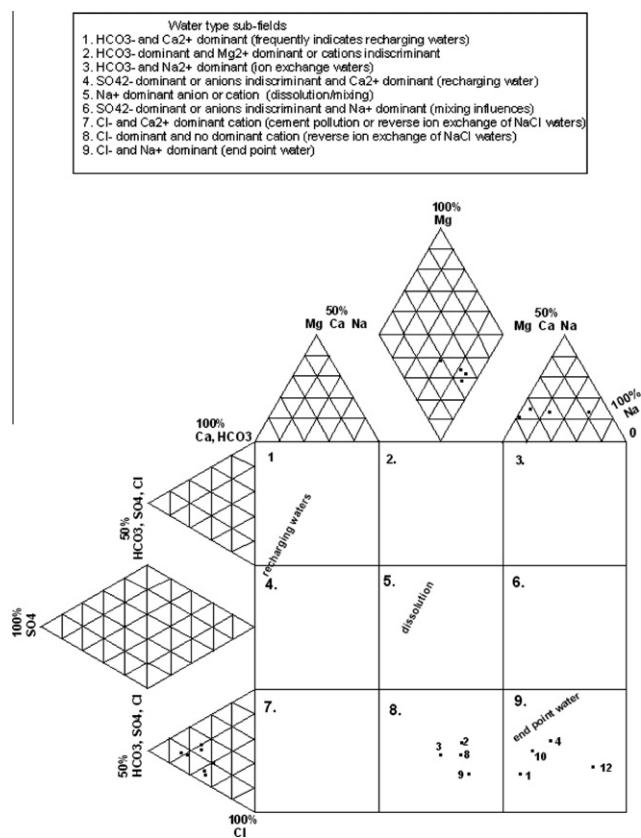


Figure 14 Durov diagram (expanded) of groundwater samples.

irrigation in most soils and requires special soil management, good drainage, high leaching and organic matter additions.

On the other hand, the remaining groundwater samples nos. 1, 3, 5, 8 and 9 having high salinity and their EC are more than 5000 ($\mu\text{mhos/cm}$). So these samples lie out of the diagram.

4.6. Conclusions

1. In the study area, the Lower Cretaceous sandstone aquifer (Malha sandstone aquifer) is main source for groundwater.
2. The aquifer parameters (effective porosity, transmissivity and hydraulic conductivity) increase due northeast with an increase of the sand percentage.

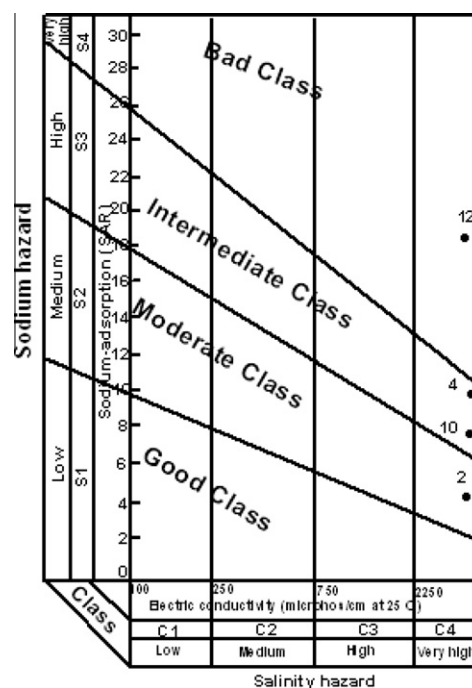


Figure 15 Classification of groundwater for irrigation (according to US Salinity Laboratory Staff Method, 1954), Lower Cretaceous aquifer.

3. The groundwater salinity for this aquifer reveals an increasing of groundwater salinity due central of study area coinciding with groundwater flow.
4. Evaluation of the concerned aquifer is achieved in the present work depending upon the new hydrogeological data for 14-drilled wells as well as hydrochemical analyses of some groundwater samples.

4.7. Recommendations

The cost of the extracted groundwater from the Lower Cretaceous sandstone aquifer is very expensive due to the pumps being installed at high depth ranging from 200 to 300 m below ground surface. It is recommended putting this groundwater to the best uses.

References

- Ali, O.F., 2006. Hydrogeological studies on Lower Cretaceous rocks (Nubia sandstone aquifer) in Central Sinai, Egypt. Ph.D. Thesis, Fac. Sci., Azhar University, Egypt, 282pp.
- Archie, G.E., 1942. The electric resistivity logs and an aid in determining some reservoir characteristics. *Petrol. Technol.* 5, 54–62.
- Continental Oil Company (CONOCO), 1987. Geologic map of Egypt (Scale 1:500,000).
- Cooper, H.H., Jacob, C.E., 1946. A generalized graphical method for evaluating formation constants and summarizing well history. *Geophys. Union Trans.* 27, 526–534.
- Durov, S.A., 1948. Natural waters and graphic representation of their compositions. *Dokl. Akad. Nauk. SSSR* 59, 87–90.
- El-Ghazawi, M.M., 1989. Hydrogeological studies in northeast of Sinai, Egypt. Ph.D. Thesis, Fac. Sci., Mansoura Univ., Egypt, 290pp., York, 377pp.
- El-Shazly, E.M., Abdel Hady, M.A., El Ghawaby, M.A., El Kassar, I.A., El Shazly, M.M., Salman, A.B., El-Rakaiby, M., 1974. Geology of Sinai Peninsula from ERTS-1 Satellite Images. ASRT, Remote Sensing Project, Cairo, Egypt, 20pp.
- Hammad, F.A., 1980. Geomorphological and hydrogeological aspects of Sinai Peninsula. *Ann. Geol. Surv. Egypt* 10, 807–817.
- Hassanin, A.M., 1997. Geological and geomorphological impacts on the water resources in Central Sinai. Ph.D. Thesis, Fac. Sci., Ain Shams Univ., Egypt, 373pp.
- Kruseman, G.P., de Ridder, N.A., 1990. Analysis and Evaluation of Pumping Test Data, second ed. Inter. Instit. Land Recl. Improv., The Netherlands, 377pp.
- Marotz, G., 1968. Technische grundlageneiner wasserspeicherung im natürlichen untergrund habilitationsschrift. Universität Stuttgart. National Academy of Science and National Academy Engineering, 1972. Water Quality Criteria. Protection Agency, Washington, DC, 594pp.
- Said, R., 1962. The Geology of Egypt. Elsevier Publishing Co., Amsterdam, New York, 377pp..
- Said, R., 1971. Explanatory notes to accompany the geological map of Egypt. *Egypt Geol. Surv. Paper* 56, 123pp.
- Said, R. (Ed.), 1990. The Geology of Egypt. A.A. Balkema Pub., Rotterdam, 734pp.
- Shata, A., 1956. Structural development of Sinai Peninsula, Egypt. *Bull. Inst. Desert Egypte* 6 (2), 117–157.
- Shata, A., 1960. The geology and geomorphology of El-Qusaima area. *Bull. Soc. Geograph. Egypte*, 95–146.
- US Salinity Laboratory Staff, 1954. Diagnosis and improvement of saline and alkali soils. Handbook No. 60. U.S. Dept. Agr., Washington, DC, 160pp.
- World Health Organization (WHO), 1993. Guidelines for Drinking Water Quality. World Health Organization, Geneva.
- Water Resources Research Institute (WRRI), 1995. Annual Hydrological Report, Internal Report, El-Qanater El Khayria, Cairo, Egypt.
- Water Resources Research Institute (WRRI), 2001. Annual Hydrological Report, Internal Report, El-Qanater El Khayria, Cairo, Egypt.
- Youssef, M.S., El-Saady, M.N., 1964. Relation between ground-water composition and geology of Dakhla Oasis. *Bull. Geogr. Egypt T*, 101–112.